Dyes and Pigments 93 (2012) 1434–1440

Contents lists available at SciVerse ScienceDirect

Dyes and Pigments

journal homepage: www.elsevier.com/locate/dyepig

Methyl orange (C.I. acid orange 52) as a new organic semiconductor: Conduction mechanism and dielectrical relaxation

I.S. Yahia [a,*], M.S. Abd El-sadek [b,c], F. Yakuphanoglu [d,e]

[a] Nano-Science Lab., Physics Department, Faculty of Education, Ain Shams University, Roxy, Cairo, Egypt
[b] Nanomaterials Laboratory, Physics Department, Faculty of Science, South Valley University, Qena, Egypt
[c] Department of Chemical Physics, Lund University, SE-22 100 Lund, Sweden
[d] Department of Physics, Faculty of Science, Firat University, 23169 Elazig, Turkey
[e] Department of Physics and Astronomy, College of Science, King Saud University, Riyadh, Saudi Arabia

ARTICLE INFO

Article history:
Received 9 February 2011
Received in revised form
30 September 2011
Accepted 3 October 2011
Available online 19 October 2011

Keywords:
Organic semiconductor
Methyl orange
Impedance spectroscopy
Conduction mechanism
CBH model
Dielectrical relaxation mechanism

ABSTRACT

The structural, electrical and dielectrical properties of the methyl orange (MO) have been investigated by X-ray diffraction and thermal analysis methods. The electrical conduction and dielectrical relaxation mechanisms of the organic compound at various frequencies and temperatures were analyzed by impedance spectroscopy. The direct current (DC) electrical conductivity confirmed that methyl orange is an organic semiconductor with calculated electronic parameters. The alternating current (AC) electrical conductivity of the sample is controlled by the correlated barrier hopping (CBH) conduction mechanism. The values of the activation energy, the density of states and the binding energy for the alternating current mechanism were determined. The real and imaginary (Z' and Z'') parts of the impedance were found to be a frequency dependence. It was found that Cole–Cole plots of the sample confirm the existence of a temperature-dependent non-Debye relaxation mechanism.

1. Introduction

Organic semiconductors have attracted research interest due to their unique electrical and optical properties and have opened many opportunities for electronic and optoelectronic device applications. A considerable amount of work has been devoted to organic materials, allowing a better understanding of their properties as well as the physical processes, which take place in materials and devices. Meanwhile, commercial products making use of organic materials have started to appear in the market, especially in the field of display flat screens [1,2] (car radios, digital cameras, cell phones, computers and televisions). The word "organic semiconductors" include polymers and low-molecular weight organic materials. The optical and electrical properties of such materials have been studied for many years [3,4]. Because of their particular structure, several peculiar physical processes may take place in organic semiconductors while these effects are less or much less significant in inorganic materials. Conversely, several concepts in standard semiconductors lose their meaning in the organic field.

Methyl orange is an intensely colored compound used in dyeing and printing textiles. It is also known as C.I. Acid Orange 52, C.I.13025, helianthine B, Orange III, Gold orange, and Tropaeolin D. Chemists use methyl orange as an indicator in the titration of weak bases with strong acids. It changes from red (at pH 3.1) to orange-yellow (at pH 4.4). Nowadays, dyeing materials are widely used in semiconductor devices due to their stability, having a conjugate structure and being rich in π-electrons [5]. Azo compounds are usually yellow or orange color, since their main absorption band in the visible spectrum is typically in the blue region. Methyl orange (MO) has a drastic change in its color (from orange to red) is easily observed as the pH of its aqueous solution changes in a narrow range of values (namely, from 3.1 to 4.4), and hence, this compound is commonly used as a convenient indicator for the titration of strong acids by weak bases. In fact, the characteristic bright colors of MO make it an important dye for the paint, textile, and photographic industries [6,7].

Thus, it is important to reveal the semiconducting properties of methyl orange as a new semiconductor material for its possibility electronic device applications. In the present work, the structural,

* Corresponding author. Tel.: +20 182848753; fax: +20 22581243.
E-mail addresses: dr_isyahia@yahoo.com, dr_isyahia@hotmail.com, isyahia@gmail.com (I.S. Yahia).

0143-7208/$ – see front matter © 2011 Elsevier Ltd. All rights reserved.
doi:10.1016/j.dyepig.2011.10.002

DC and AC conductivities of methyl orange (MO) that formed in pellet shape have been investigated. The structural characterization, the conduction mechanism and the relaxation process of methyl orange have been done using X-ray diffraction, thermal analysis and impedance spectroscopy.

2. Experimental detail

Methyl orange as shown in scheme 1 was purchased from Aldrich Company with high purity. MO powder was formed in the shape of pellet by applying 5 ton by using a hydraulic press. The diameter of the pellets for DC and AC measurements is equal to 13 mm and its thickness equals to 1 mm.

The real (Z') and imaginary (Z'') parts of the impedance Z at different temperatures were directly measured by a computer controlled HIOKI 3532-50 LCR meter. DC electrical conductivity of the sample was measured by a Keithley 6517 A electrometer. A special designed holder was used to study the DC and AC measurements. The present study covered a temperature range from 293 to 523 K. The temperature of the highly shielded home-made furnace controlled via type K thermocouple directly connected to a temperature controller. Powder X-ray diffraction (XRD) analysis of MO was carried out with a Philips model X'pert diffractometer with *CuKα* radiation operated at 30 kV and 25 mA with CuK_α ($\lambda = 0.15406$ nm) radiation.

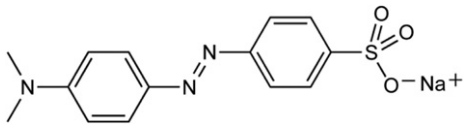

Scheme. 1. The molecular structure of methyl orange.

3. Results and discussion

3.1. X-ray diffraction and thermogravimetry analysis

The structural properties of methyl orange powder were investigated by X-ray diffraction (XRD) pattern, as shown in Fig. 1. XRD results indicate that the methyl orange (MO) has a polycrystalline nature. The cell parameters values of MO sample were indexed and refined using crsyfire and checkcell software [8]. X-ray diffraction (XRD) powder pattern of methyl orange indicates that MO sample has a triclinic structure with the unit cell parameters as: $a = 7.0072$ Å, $b = 11.5637$ Å, $c = 16.8413$ Å, $\alpha = 54.34°$, $\beta = 70.33°$ and $\gamma = 85.94°$.

Thermal analysis plays an important role in determining thermal stability of the organic material. The TG curve, as shown in Fig. 2 reveals that the methyl orange decomposes in three steps in the studied temperature range (RT-800 °C). MO is a stable organic semiconductor through a wide range of temperature.

3.2. Electrical properties of the methyl orange

The direct current electrical conductivity dependence of temperature of the methyl orange is shown in Fig. 3. The DC conductivity increases with increasing temperature. The variation of electrical conductivity with temperature was analyzed by the following equation [9,10]:

$$\sigma_{DC} = \sigma_{o1}\exp\left(-\frac{\Delta E_1}{kT}\right) + \sigma_{o2}\exp\left(-\frac{\Delta E_2}{kT}\right) \quad (1)$$

where σ_{o1} and σ_{o2} are the pre-exponential factor for region I and II, respectively, k is the Boltzmann's constant, ΔE_1 and ΔE_2 are the DC conduction activation energy for region I and II, respectively. The values of ΔE_1 and ΔE_2 were calculated from the slopes of the obtained straight lines indicating that there are two conduction mechanisms in the studied range of temperature. The values of DC activation energy and the pre-exponential term were determined using the least-squares fitting of the experimental data via origin software. The values ΔE_1 and σ_{o1} for region (I) were found to be 0.540 eV, and 0.072 $(\Omega\ m)^{-1}$, respectively and the values ΔE_2 and σ_{o2} for region (II) were determined to be 0.837 eV and 663.81 $(\Omega\ m)^{-1}$, respectively. The calculated activation energy values are lower than half of the optical energy gap as in intrinsic semiconductors. The electrical conductivity results indicate that the electrical conduction mechanism is a thermally-activated process and that the DC electrical conductivity increases exponentially over the studied range of temperatures [9,10]. The electrical conductivity of the MO sample increased with increasing

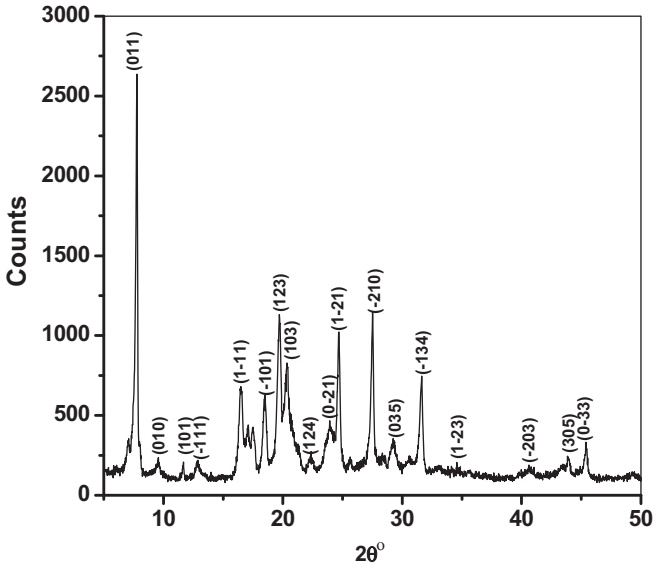

Fig. 1. XRD pattern of methyl orange.

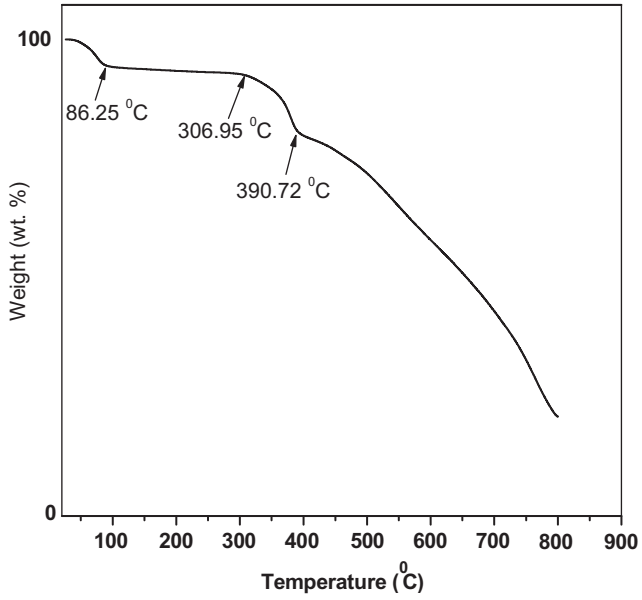

Fig. 2. TGA pattern of methyl orange.

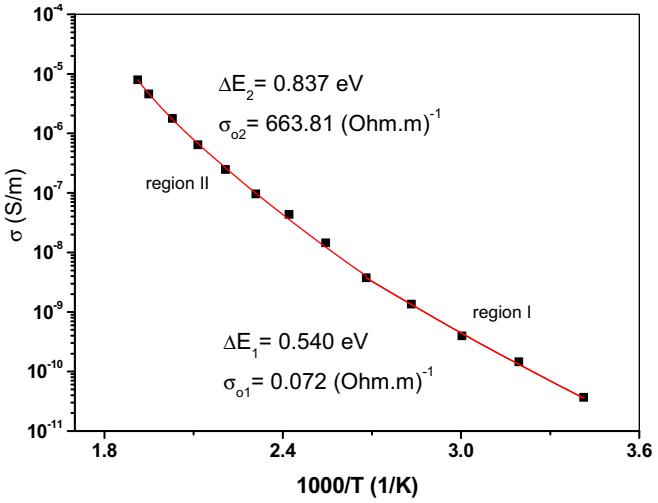

Fig. 3. Semi-logarithmic plot of the temperature dependence of the DC electrical conductivity for methyl orange.

temperature indicating that the electrical conduction mechanism is similar to that of semiconductors. The obtained electronic parameters confirm that MO is an organic semiconductor dye [11,12]. This semiconducting behavior results from the transfer of π-electrons. Electronic excitation of the benzene ring follows the transfer of an electron to another molecule. Resonance stabilization is started by moving of an unshared electron pair from an oxygen atom to a benzene ring, caused by temporary sharing of π-electrons by oxygen and carbon. The lone pair of electrons on an oxygen atom with a π-bond allows delocalization of the π-electrons [12,13].

3.3. Temperature dependence of the AC electrical conductivity

The temperature dependence of the AC conductivity $\sigma_{AC}(\omega)$ of the sample at a particular frequency and temperature is shown in Fig. 4 and it can be defined as [14,15]:

$$\sigma_{Tot.AC}(\omega) = \sigma_{AC}(\omega) + \sigma_{DC}(\omega \rightarrow 0) \quad (2)$$

where ω is the angular frequency. The first part is a frequency and temperature-dependent term which is related to the dielectric relaxation of the bound charge carriers and the second part represents the DC conductivity which is related to the drift mobility of the free charge carriers. This accounts for the free charges resident in the bulk and is independent of the frequency [14,15]. At lower temperatures, the total AC conductivity shows weak temperature dependence and is substantially higher than DC conductivity. However, at higher temperatures, the temperature dependence becomes stronger and the variation with frequency is small. It is clear from Fig. 5 that $\ln\sigma_{AC}(\omega)$ increases nonlinearly with the temperature. If $\ln\sigma_{AC}(\omega)$ depends linearly on the temperature with single activation energy, the mechanism is due to the hopping between states near the mobility edges, where the density of states is taken to be constant but the obtained dependence is not linear. A possible explanation of this behavior is that the density of states rises continuously toward the band edges [14,15]. Rockstad and Elliott have expressed the AC conductivity as [16,17]:

$$\sigma_{AC}(\omega) = \sigma_W + \sigma_S \quad (3)$$

Here, σ_W represents the weak temperature-dependent mechanism, which has been interpreted as being due to bipolaron hopping between D^+ and D^- centers. While, σ_S represents the strong temperature-dependent mechanism, which has been interpreted as being due to excitation to the localized states at the band edges, where the conduction takes place by quantum mechanical tunneling. A single polaron hopping has been accounted at higher temperatures mechanism. At the higher temperatures, the increase of the density of neutral defects D^0 is important and CBH of single polarons, which are holes hopping between D^0 and D^- and electrons between D^0 and D^+, is the dominant contribution to AC conduction in different materials [18,19].

This temperature dependence of AC conductivity suggests that it is a thermally-activated process and it can be interpreted according to Arrhenius equation [20–22]:

$$\sigma_{AC}(\omega) = \sigma_o \exp\left(\frac{-\Delta E(\omega)}{kT}\right) \quad (4)$$

where σ_o is constant and $\Delta E(\omega)$ is the activation energy for AC electrical conduction mechanism. The activation energy for AC

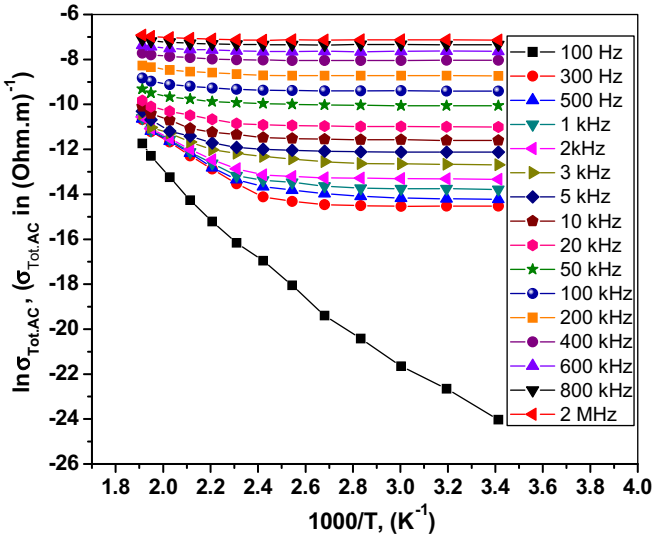

Fig. 4. Temperature dependence of the calculated total electrical conductivity $\sigma_{Tot.AC}(\omega)$ for methyl orange.

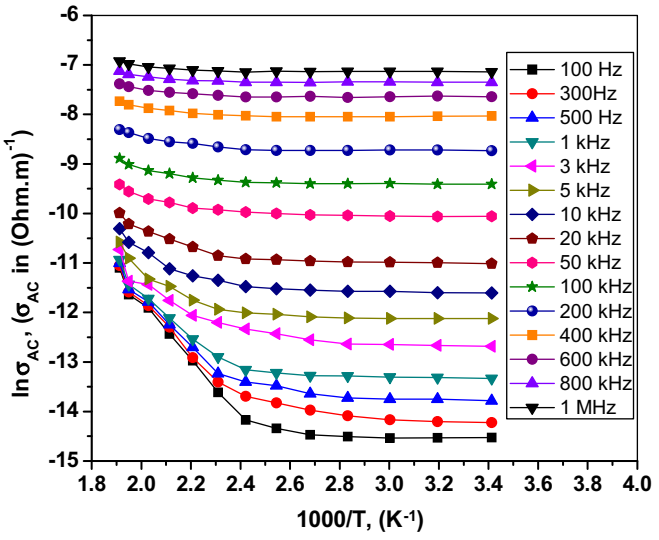

Fig. 5. Temperature dependence of the AC electrical conductivity $\sigma_{AC}(\omega)$ for methyl orange.

conduction for the various frequencies at higher temperature range was calculated from the slopes of the straight lines of Fig. 5. The frequency dependence of the AC activation energy $\Delta E(\omega)$ of methyl orange is shown in Fig. 6. It is clear that the value of $\Delta E(\omega)$ is almost constant at the lower frequencies and then sharply decreased with the further increasing of the applied frequency. Such behavior can be attributed to the contribution of the frequency to the conduction mechanism, which confirms that the hopping conduction is the dominant conduction mechanism in this compound. The increase of frequency enhances the electronic jumps between the localized states, and consequently the activation energy $\Delta E(\omega)$ decreases with increasing frequency [20,21]. The obtained activation energy is extremely low and it changes slightly with frequency. The low value of activation energy indicates that the electric conduction in this material is taken place by hopping of charge carriers between the defect states near the Fermi level. The charge transfer involves transitions of bipolarons from the defect levels D^- and D^+, whereas the participation of neutral centers D^0 in conduction is negligible in the investigated temperature range [22].

Fig. 7 shows the relation between $\ln\sigma_{AC}(\omega)$ and $\ln(\omega)$ for methyl orange (MO) at the temperature range of 293–523 K. A common feature in ordered, disordered, inorganic and organic semiconductors is a frequency dependence of the AC conductivity that increases approximately linearly with frequency. The AC conductivity of the sample can be expressed according to the following equation [23]:

$$\sigma_{AC}(\omega) = A\omega^s \tag{5}$$

where s is the frequency exponent and A is the constant dependent on temperature. The frequency dependent exponent is characteristic parameter representing the many body interactions of the electrons, charges and impurities. It depends on the material temperature T and varies from 0 to 1; for ideal Debye type samples it is equal to 1. The exponent s associated with the charge carriers or with extrinsic dipoles arises from presence of defects or impurities. The power law dependence of AC conductivity on the frequency has a universal nature and corresponds to the short range hopping of charge carriers through the trap sites that are separated by energy barriers of varied heights [24]. The values of the frequency exponent s at different temperature values were calculated for methyl orange (MO), from the slopes of linear part of the relation of $\ln\sigma_{AC}(\omega) = (\omega)$ at the higher frequency range. It is clear from theses plots that at a certain point of the applied frequency, the conductivity increases linearly with increasing the applied frequency. It is clear that the DC contribution is important at lower frequencies and whereas, at higher temperatures, the frequency dependent term dominates at higher frequencies. Also, in the lower frequency region, the conductivity depends on temperature. Such dependence may be described by the variable range hopping (VRH) mechanism. The VRH model is frequency independent and only weakly temperature dependent compared to the band theory and this model is important for the electrical conduction mechanism of the organic semiconducting materials [9,25]. The values of exponent s for methyl orange at different temperatures were calculated from the slopes of the linear parts of the relation of $\ln\sigma_{AC}(\omega) = (\omega)$ at higher frequencies. The temperature dependence of s for the sample is shown in Fig. 8. As seen in Fig. 8, the s values decrease as the temperature increases for the studied sample. According to the correlated barrier hopping CBH model [20–22], the frequency exponent s can be defined by the relation:

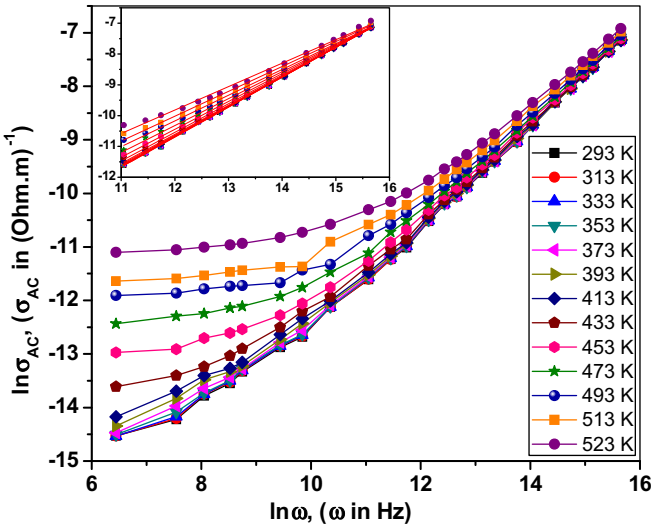

Fig. 7. Frequency dependence of AC electrical conductivity for methyl orange at different temperatures.

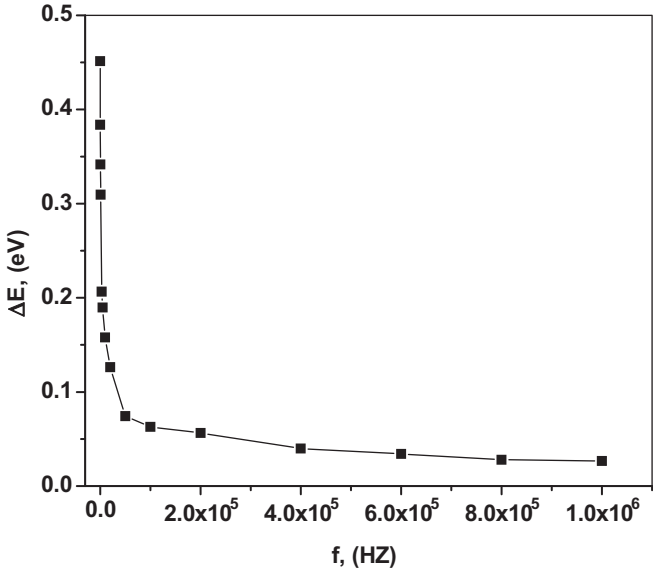

Fig. 6. Frequency dependence of the AC activation energy $\Delta E(\omega)$ for methyl orange.

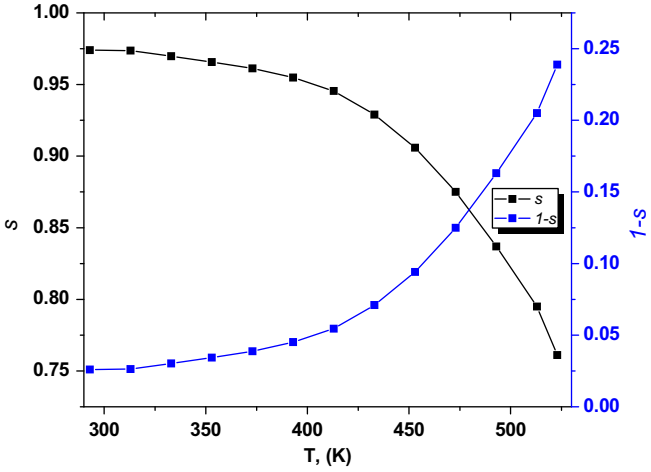

Fig. 8. Temperature dependence of the frequency exponent s and $1 - s$ for methyl orange.

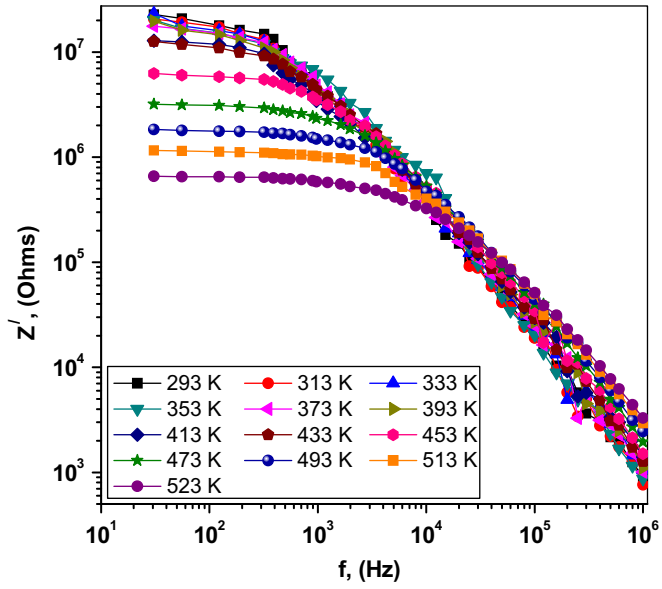

Fig. 9. Log–log plot of the real part of impedance as a function of frequency for methyl orange at different temperatures.

$$s = 1 - \frac{6kT}{W_M + [kT\ln(\omega\tau_0)]} \tag{6}$$

The obtained data for s satisfy to Eq. (6) and thus, the frequency dependence of $\sigma_{AC}(\omega)$ can be explained satisfactorily in terms of the CBH model [20]. The binding energy W_m can be defined as the binding energy of the carrier in its localized sites. The binding energy W_m is related to the maximum barrier height at infinite interstatic separation, which is called the polaron binding energy, i.e. the binding energy of the carrier in its localized site. The values of $1 - s$ were plotted as function of temperature T, as shown in Fig. 7 and its slope is used to calculate the binding energy W_m and it was found to be 0.304 eV.

According to the Austin–Mott formula [26] based on CBH model, AC conductivity $\sigma_{AC}(\omega)$ can be explained in terms of hopping of electrons between a pair of localized states $N(E_F)$ at the Fermi level E_F. $\sigma_{AC}(\omega)$ is related to the number of sites per unit energy per unit volume $N(E_F)$ at the Fermi level as given by:

$$\sigma_{AC}(\omega) = \left(\frac{\pi}{3}\right)[N(E_F)]^2 Tk_B e^2 \alpha^{-5} \omega \left[\ln\left(\nu_{ph}/\omega\right)\right]^4 \tag{7}$$

where α is the exponential decay parameter of localized states wave functions ($\alpha^{-1} = 10$ Å), ν_{ph} is the characteristic phonon

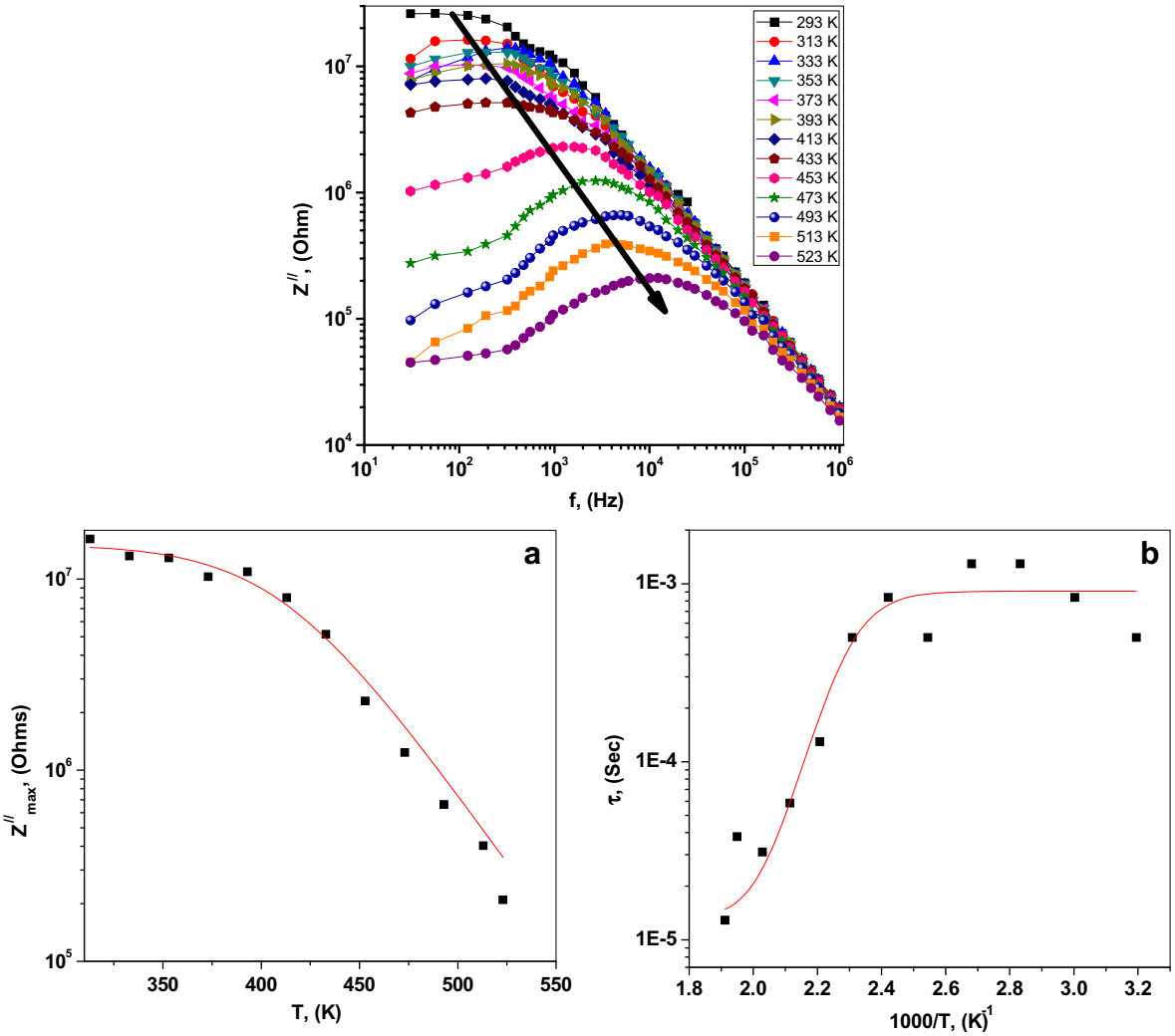

Fig. 10. Log–log plot of the imaginary part of impedance as a function of frequency for methyl orange at different temperatures. (a) Semi-logarithmic plot of Z'_{max} as a function of temperatures for methyl orange. (b) Semi-logarithmic plot of the relaxation time as a function of temperatures for methyl orange.

frequency ($\nu_{ph} = 10^{12}$ s^{-1}) and $N(E_F)$ is the density of states near the Fermi level. The density of localized states $N(E_F)$ was determined using Eq. (7) at different temperatures and frequencies. The values of $N(E_F)$ are of order of 5.98–7.52 $\times$ 10^{21} eV^{-1} cm^{-3} in the studied range of temperatures and frequencies. The values of $N(E_F)$ increase with temperature, confirming that the electrical conductivity increases with temperature.

3.4. Impedance spectroscopy studies of methyl orange

Complex impedance spectroscopy can be analyzed using four different complex equations as follows [27–29]:

$$Z^*(\omega) = Z' - jZ'' = R_s + \frac{j}{\omega C_s} \tag{8}$$

where

$$Z = R_s + \frac{R_p - j\omega R_p^2 C_p}{1 + \omega^2 R_p^2 C_p^2} \tag{9}$$

$$Z' = R_s + \frac{R_p}{1 + \omega^2 R_p^2 C_p^2} \tag{10}$$

$$Z'' = \frac{\omega R_p^2 C_p}{1 + \omega^2 R_p^2 C_p^2} \tag{11}$$

where R_s is the series resistance, R_p is the parallel resistance C_p is the parallel capacitance and ω is the angular frequency $\omega = 2\pi f$. These data can also be presented as a complex plot, i.e., the imaginary versus real component with variable frequency or real and/or imaginary components as a function of log f.

The electrical properties of the materials have been investigated using impedance spectroscopy. Fig. 9 shows the variation of the real part of the impedance (Z') as a function of frequency at different temperatures and it shows a monotonous decrease in the value of (Z') with increasing temperature and the curves almost merge for all temperatures at the higher frequency region ($\geq$10 kHz) for the studied sample. The decrease in (Z') with increase in temperature and frequency indicates the possibility of an increase in AC conductivity with increasing temperature and frequency [30,31]. Further, the (Z') values show a negative temperature coefficient of resistance (NTCR) type behavior for the sample [28,32].

Fig. 10 shows the variation of the imaginary part of the impedance (Z'') with frequency at different temperatures as loss spectrum. The plot of (Z'') exhibits a decrease in its values with asymmetric peak broadening shifted to the higher frequencies. The plots of (Z'') with an asymmetric broadening of peaks indicate the existence of a temperature-dependent electrical relaxation phenomenon for this sample [28,33]. The values of Z'_{max} decrease and shift to the higher frequencies with the increase of temperature, as shown in Fig. 10(a). The maximum frequency f_{max}, called the relaxation frequency, was determined to calculate the relaxation time τ and it is independent of the sample geometrical factors and depends basically on the intrinsic properties of the material sample. The values of τ were determined from the maximum peak positions of Fig. 10 using $\omega\tau = 2\pi f_{max}\tau = 1$. The variation of τ as a function of temperature is shown in Fig. 10b. This pattern shows that the relaxation time decreases as the temperature increases. This result indicates the presence of temperature-dependent electrical relaxation phenomena for the sample. The relaxation time is decreased due to the dipoles following the motion of the alternating field due to the dissipated thermal energy [28,33].

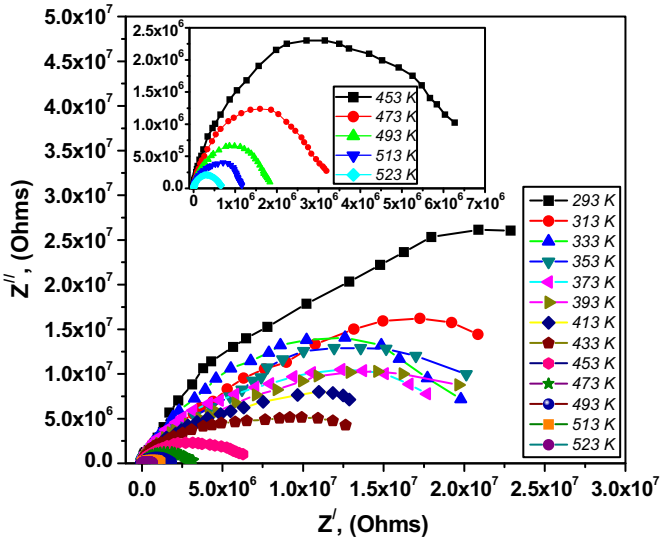

Fig. 11. Complex impedance plots of methyl orange at different temperatures.

Fig. 11 shows the Cole–Cole plot of methyl orange at various temperatures. The inset: represents the variation of the plot in the temperature range (453–523 K) for better illustration. It can be also seen in Fig. 11 that the complex impedance data are represented by depressed semicircle (i.e., centers of semicircle lie below the abscissa axis). This indicates the presence of a non-Debye dielectric relaxation for the sample. This behavior suggests the temperature-dependent hopping type of mechanism for electric conduction in the studied sample. The impedance spectra are characterized by the appearance of a single semicircular arc whose radii of curvature decreases with increasing temperature. The intercepts of the semicircular arcs with the real axis Z' were used to determine the bulk resistance R_b of the material. The bulk resistance is given by [28]:

$$R_p = R_o \exp\left(\frac{\Delta E_{R_b}}{k_B T}\right) \tag{12}$$

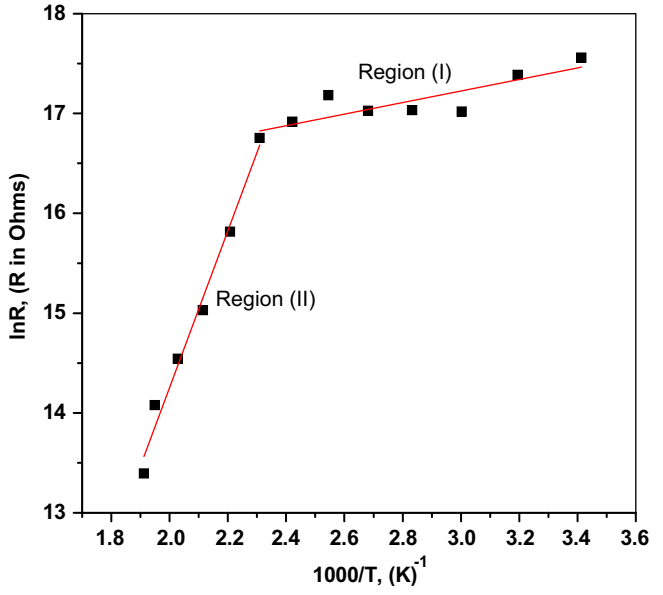

Fig. 12. Variation of bulk resistance as a function of temperatures for methyl orange.

where ΔE_{R_b} is the activation energy and R_o is a constant. $\ln R_b$ was plotted as a function of a reciprocal temperature, as shown in Fig. 12. This plot indicates that there are two conduction regions with two activation energies. It can be seen that the bulk resistance decreases with the increase of temperature showing a typical semiconducting property, i.e. negative temperature coefficient of resistance (NTCR) behavior. The values of R_o and ΔE_{R_b} are 6.23×10^6 Ω and 0.046 eV for region (I) and 0.237 Ω and 0.677 eV for region (II), respectively.

4. Conclusion

The X-ray diffraction (XRD) powder pattern of methyl orange shows that MO has a triclinic structure with the unit cell parameter, $a = 7.0072$ Å, $b = 11.5637$ Å, $c = 16.8413$ Å. DC electrical conductivity shows that MO is an organic semiconductor with calculated electronic parameters. The AC conductivity of the sample can be reasonably interpreted in terms of the correlated barrier hopping (CBH) model. The variation of Z'' with the increase of temperature suggests a negative temperature coefficient of resistance (NTCR) type behavior. The Cole–Cole plots indicate the existence of a temperature-dependent electrical relaxation phenomenon for the MO sample. The dielectric relaxation mechanism of the sample exhibits a non-Debye-type dielectric relaxation. It is evaluated that the methyl orange is an organic semiconductor with a wide range of thermal stability and it can be a good candidate in dielectric and semiconductor devices.

References

[1] Burroughes JH, Bradley DDC, Brown AR, Marks RN, Mackay K, Friend RH. Light-emitting diodes based on conjugated polymers. Nature 1990;347:539–41.
[2] Nguyen TP, Destruel P. In: Nalwa HS, Rohwer LS, editors. Handbook of luminescence and display materials and devices, vol. 1. American Scientific Publishers; 2003.
[3] Pope M, Swenberg CE. Electronic processes in organic solids. Oxford: Oxford University Press; 1982.
[4] Kao KC, Hwang W. Electrical transport in solids. Oxford: Pergamon Press; 1981.
[5] http://antoine.frostburg.edu/chem/senese/101/acidbase/faq/methyl-orange.shtml.
[6] Sanchez AM, Barra M, De Rossi RH. On the mechanism of the acid/base-catalyzed thermal cis–transisomerization of methyl orange. J Org Chem 1999;64:1604–9.
[7] Azuki M, Morihashi K, Watanabe T, Takahashi O, Kikuchi O. Ab initio GB study of the acid-catalyzed cis–trans isomerization of methyl yellow and methyl orange in aqueous solution. J Mol Struct THEOCHEM 2001;542:255–62.
[8] Farag AAM, Yahia IS. Rectification and barrier height inhomogeneous in Rhodamine B based organic Schottky diode. Synth Metals 2011;161:32–9.
[9] Mansour Sh A, Yahia IS, Yakuphanoglu F. The electrical conductivity and dielectric properties of C.I. Basic Violet 10. Dyes Pigments 2010;87:144.
[10] Mansour Sh A, Yahia IS, Sakr GB. Electrical conductivity and dielectric relaxation behavior of fluorescein sodium salt (FSS). Solid State Commun 2010;150:1386–91.
[11] Yakuphanoglu F, Sekerci M, Evin E. The determination of the conduction mechanism and optical band gap of fluorescein sodium salt. Physica B 2006;382:21.
[12] Yakuphanoglu F, Erol I. A novel organic semiconducting material: 2-(3-mesityl-3-methylcyclobutyl)-2-keto-ethyl methacrylate (MCKEMA). Physica B 2004;352:378.
[13] Hassib H, Abdel Razik A. Dielectric properties and AC conduction mechanism for 5,7-dihydroxy-6-formyl-2-methylbenzo-pyran-4-one bis-schiff base. Solid State Commun 2008;147:345.
[14] Elliott SR. A.C. conduction in amorphous chalcogenide and pnictide semiconductors. Adv Phys 1987;36:135.
[15] Mott NF, Davis EA. Electronic processes in non-crystalline materials. Oxford: Clarendon Press; 1971.
[16] Elliott SR. Temperature dependence of A.C. conductivity of chalcogenide glasses. Philos Mag B 1978;37:553.
[17] Bilen Bukem, Skarlatos Yani, Aktas Gulen. Frequency-dependent conductivity in As_2Se_3 and As_2Te_3 thin films. J Non-Crystalline Solids 2005;351:2153–8.
[18] Ghosh A. Transport properties of vanadium germanate glassy semiconductors. Phys Rev B 1990;42:5665.
[19] Shimakawa K. On the temperature dependence of a.c. conduction in chalcogenide glasses. Philos Mag B 1982;46:123.
[20] Reda SA. Electric and dielectric properties of some luminescent solar collectors based on phthalocyanines and hematoporphyrin doped PMMA. Dyes Pigments 2007;75:526.
[21] Yakuphanoglu Fahrettin, Evin Ertan, Okutan Mustafa. The dielectrical and alternating current conductivity properties of $40Cu+20Co+40Y_2O_3$ ceramic. Physica B 2006;382:285.
[22] Lukic SR, Skuban SJ, Skuban F, Petrovic DM, Tveryanovich AS. DC and AC conductivities of $(As_2S_3)_{100-x}(AsSe0.5Te0.5I)_x$ chalcogenide glasses. Physica B 2008;403:2578.
[23] Jonscher AK. The 'universal' dielectric response. Nature 1977;267:673.
[24] Jali VM, Aparna S, Sanjeev Ganesh, Krupanidhi SB. AC conductivity studies on the electron irradiated $BaZrO_3$ ceramic. Nucl Instruments Methods Phys Res B 2007;257:505.
[25] Yakuphanoglu F, Yahia IS, Barim G, Filiz Senkal B. Double-walled carbon nanotube/polymer nanocomposites: electrical properties under dc and ac fields. Synth Metals 2010;160:1718.
[26] Austin IG, Mott NF. Polarons in crystalline and non-crystalline materials. Adv Phys 1969;18:41.
[27] Macdonald JR. Impedance spectroscopy: emphasizing solid materials and systems. New York: Wiley; 1987.
[28] Chandra KP, Prasad K, Gupta RN. Impedance spectroscopy study of an organic semiconductor: alizarin. Physica B 2007;388:118–23.
[29] Vishal Shrotriya, Yang Yang. Capacitance–voltage characterization of polymer light-emitting diodes. J Appl Phys 2005;97:054504.
[30] Ashok Kumar, Singh BP, Choudhary RNP, Thakur Awalendra K. A.C. impedance analysis of the effect of dopant concentration on electrical properties of calcium modified $BaSnO_3$. J Alloys Compounds 2005;394:292–302.
[31] Selvasekarapandian S, Vijaykumar M. The ac impedance spectroscopy studies on $LiDyO_2$. Mater Chem Phys 2003;80:29–30.
[32] James AR, Srinivas K. Low temperature fabrication and impedance spectroscopy of PMN-PT ceramics. Mater Res Bull 1999;34:1301.
[33] Suman CK, Prasad K, Choudhary RNP. Impedance spectroscopic studies of ferroelectric $Pb_2Sb_3DyTi_5O_{18}$ ceramic. Adv Appl Ceram 2005;104:294.